CHANDRA
X-ray Center   60 Garden St., Cambridge Massachusetts 02138 USA

Date: January 27, 2017
From: John ZuHone, Herman Marshall, Richard Edgar, & Paul Plucinsky
To: Chandra Operations Team
Subject: Estimation of Potential Polymerization of ACIS OBF Contaminant

1   Abstract

A contamination layer has built up on the ACIS Optical Blocking Filters over the lifetime of the *Chandra* mission. A bakeout of the ACIS instrument could potentially drive the contaminant off the filters, but this might be difficult if the contaminant has been significantly polymerized by exposure to ultraviolet light. This memo is presented to support the conclusion that the filters have been exposed to insufficient ultraviolet light over the duration of the mission to significantly polymerize the contaminant.

2   Introduction

It was noticed early in the mission that the low-energy sensitivity of ACIS is decreasing with time. It has been determined that the loss of effective area is due to a contamination layer building up on the surface of the Optical Blocking Filters (OBFs) facing the spacecraft interior. The contamination layer continues to accumulate even after 16 years on orbit. The accumulation rate, the chemical composition, and the spatial distribution of the contaminant have all varied with time over the mission.

In 2004, the CXO project considered a "bakeout" of the ACIS instrument to remove the contaminant, but it was decided it was not worth the risk, and shortly thereafter the accumulation rate of the contaminant decreased. However, since 2012, the rate of accumulation of the contaminant has been increasing, raising again the need to consider a possible bakeout. Figure 1 shows the increase in areal density of the contaminant as a function of time over the life of the mission so far.

One factor which would determine the likelihood of a successful bakeout is the volatility of the contaminant, which is unknown since we do not know its molecular structure. If the volatility of the contaminant is low, it will be much more difficult to bake it off. One possibility for a low volatility case is if the contaminant is significantly polymerized. After the first Hubble Space Telescope (HST) servicing mission in 1999, a layer of polymerized contaminant was discovered on the pick-off mirror of the WFPC1 camera. It was subsequently determined that the polymerization of the material occurred due to ultraviolet (UV) photons breaking molecular bonds of contaminant molecules, which subsequently
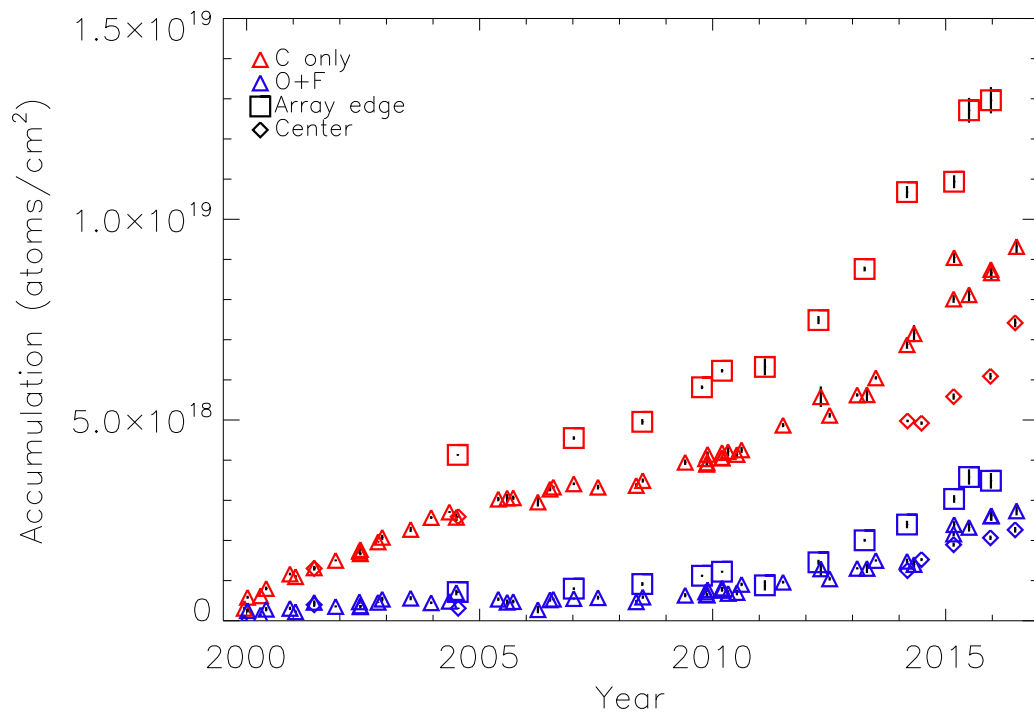
Figure 1: Areal densities of C and O+F as a function of time. The C density is plotted in red and the O+F density is plotted in blue. The different symbols indicate different locations on the filter. The diamonds are in the center, the triangles ∼1/3 from the edge, and the boxes are at the edge. Figure adapted from Plucinsky et al. 2016.

combine to form longer polymer molecules. The primary source of these UV photons was from the Sun, reflected from the bright Earth (Feinberg et al. 1995).

This implies that the contaminant that has built up on the OBFs may have been similarly polymerized by UV photons. In this memo, we perform an analysis of the various likely sources of UV flux which have impinged on the OBFs over the lifetime of the mission, to determine if there has been a fluence of UV photons with sufficient energy to polymerize a significant amount of the contaminant, which could significantly degrade the efficacy of a potential bakeout of the ACIS OBFs.

3   Estimation of the Effects of UV Fluence

In this section, we will present a series of calculations of the estimated UV fluence "observed" by ACIS from various sources. Our goal is to calculate a "worst-case" UV fluence, which will necessitate a number of simplifying assumptions. We will detail these assumptions throughout this memo, but in general we assume:

1. the HRMA is 100% reflective to UV photons

2. observations of all sources are at the same aimpoint

Neither of these assumptions are strictly true, but adopting them provides an upper limit on the UV fluence that could have impinged upon the ACIS OBFs. In particular, assumption 2 is very conservative, since observations of sources may be made with either ACIS-I or ACIS-S, and not always at the same aimpoint on either detector. In Section 3.4.1, we will relax this assumption to provide a more realistic estimate of the UV fluence from observations of Venus.

3.1   Assumptions About the Nature of the Contaminant

Since we do not know the molecular composition of the contaminant, it will also be necessary to make some further assumptions. It is known that the contaminant is composed primarily of H and C atoms, with some amounts of O and F. We will assume that the contaminant is a saturated hydrocarbon, primarily composed of covalently bonded H and C atoms, with n_C C atoms per molecule. For example, O'Dell et al. 2015 performed simulations of the vaporization of contaminant from the ACIS OBFs due to a bakeout procedure, assuming reference molecules of dioctyl phthalate ($C_{24}H_{38}O_4$, $n_C = 24$) and octadecane ($C_{18}H_{38}$, $n_C = 18$).

This indicates that H-C or C-C bonds must be broken in order to polymerize the contaminant. The energies required to break these bonds are $E_{H-C} = 99$ kcal/mol and $E_{C-C} = 83$ kcal/mol.[1] These energies correspond to photon wavelengths of $\lambda_{H-C} = 2888$ Å

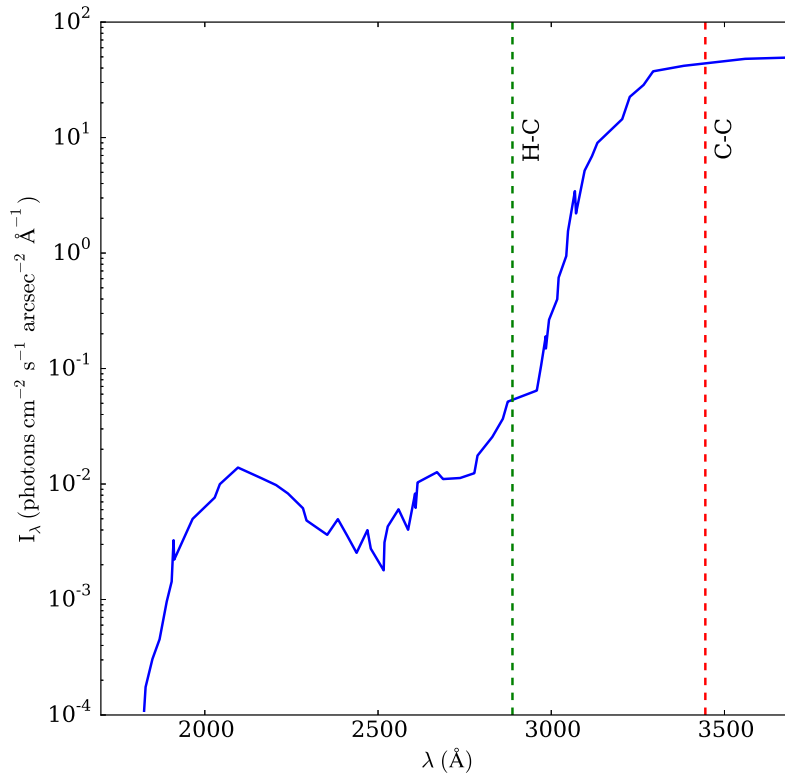[1] http://www.cem.msu.edu/~reusch/OrgPage/bndenrgy.htm

Figure 2: Specific intensity of solar UV photons backscattered from the bright earth. Dashed vertical lines show the wavelengths of photon energies that can break H-C and C-C bonds. Figure reproduced from Feinberg et al. 1995.

and $\lambda_{C-C} = 3445$ Å. We are relatively confident that there are very few C=C bonds with 146 kcal/mol, and F-C bonds are readily broken (Marshall et al. 2004), so we restrict our attention to H-C and C-C bonds.

3.2   UV Fluence from the Bright Earth

We consider first the solar UV fluence, scattered from the Earth's atmosphere. Figure 2 shows the specific intensity of these UV photons in the ~1800-3800 Å wavelength range, reproduced from Feinberg et al. 1995. There are steep drops in intensity around 1900 Å and 3000 Å. We tabulate this specific intensity and numerically integrate it over wavelength to determine that the intensity of photons which can break the H-C and C-C bonds are I_{H-C} = 9.23 photons s^{-1} cm^{-2} arcsec^{-2} (integrating between 1800 Å and 2888 Å) and I_{C-C} = 7132.04 photons s^{-1} cm^{-2} arcsec^{-2} (integrating between 1800 Å and 3445 Å).

Though *Chandra* does not directly observe the bright Earth, the telescope boresight can scan across the Earth during maneuvers. Therefore, in order to determine the total UV fluence reflected from the bright Earth which impinged upon the OBFs, it is necessary to determine the total time accumulated over the lifetime of the mission when the following two conditions are simultaneously satisfied:

1. The Earth is in the HRMA field of view

2. ACIS is in the focal plane

We assume that condition 1 is satisfied when the angular radius of the Earth is less than the angular distance between the Earth center and the aimpoint. This was determined by querying the `Ska` engineering archive for the MSIDs `Dist_SatEarth` and `Point_EarthCentAng`, corresponding to the distance between the Earth's center and *Chandra* (D_E) and the angle ϕ_E between the Earth and the aimpoint, respectively. The angular radius of the Earth θ_E is determined via $\theta_E = \tan^{-1}(R_\oplus/D_E)$. We assume that condition 2 is satisfied when the TSC position is $\geq$ -25,000. This can be determined using the MSID `3TSCPOS` from the `Ska` archive.

The time resolution of the first two MSIDs in the archive is $\Delta t = 5$ min, whereas the resolution of `3TSCPOS` is 32.8 seconds, so the time resolution of the calculation is limited to 5-minute intervals. This likely results in a modest overestimate of the total length of time that the OBFs have been exposed to the bright Earth, since the Earth will be entering and exiting the field of view during some of these intervals, and will not be within it during the entire 5 minutes. We do not seek to quantify this overestimate further, since we are adopting a "worst-case" approach to this problem. The total time ΔT during which the ACIS OBFs are exposed to the bright Earth is then calculated by simply summing the time intervals which jointly satisfy these conditions:
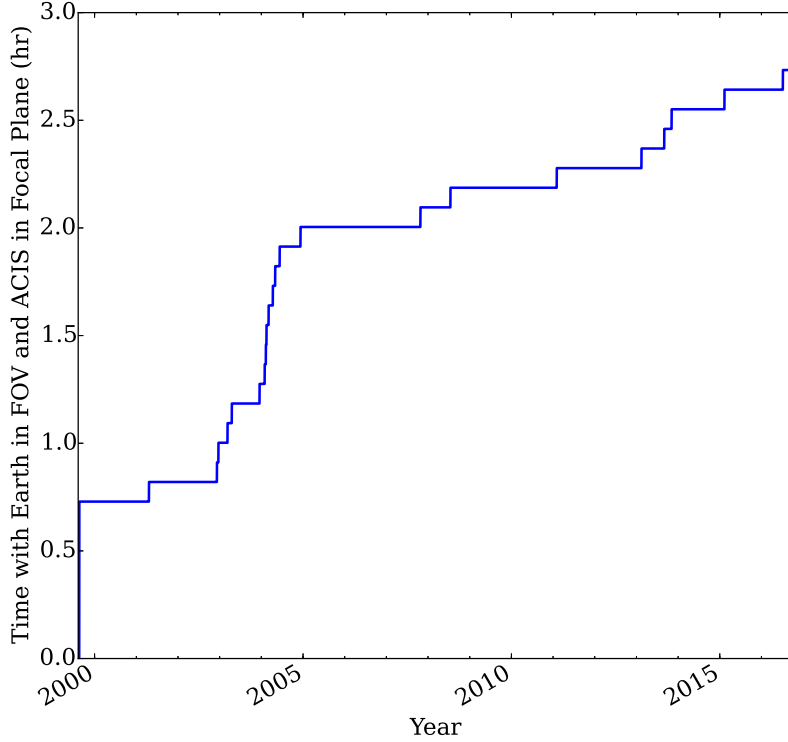
Figure 3: Accumulation of time with Earth in the FOV and ACIS in the focal plane over the duration of the mission.

$$\begin{aligned}
\Delta T &= \sum_i \Delta t_i, \text{ where } (\phi_{E,i} \leq \theta_{E,i}) \text{ and } (\texttt{3TSCPOS}_i > -25000) \qquad (1)\\
&= 2.73 \text{ hr}
\end{aligned}$$

Figure 3 shows the accumulation of this time over the duration of the mission.

As mentioned above, we assume that the UV photons are reflected from the HRMA onto the focal plane with 100% efficiency, so the effective area is $A_{\text{eff}} = 1145 \text{ cm}^2$. The "plate scale" ΔS of the ACIS focal plane is $0.0205''/\mu$m. The accumulated fluences of photons which can break H-C and C-C bonds are then, respectively:

$$\begin{aligned}
H_{\text{H-C}} &= I_{\text{H-C}} A_{\text{eff}} (\Delta S)^2 \Delta T = 4.06 \times 10^{12} \text{ photons cm}^{-2} \qquad (2)\\
H_{\text{C-C}} &= I_{\text{C-C}} A_{\text{eff}} (\Delta S)^2 \Delta T = 3.38 \times 10^{15} \text{ photons cm}^{-2} \qquad (3)
\end{aligned}$$

6

where the number of photons which can break C-C bonds is much higher due to the steep increase in intensity of these photons at wavelengths longer than ∼3000 Å (Figure 2).

We can now make a rough estimate of the amount of contaminant that could be polymerized by these photons. Assuming 100% efficiency (e.g., that each UV photon which impinges upon the OBFs breaks a bond), and that the number of photons required to polymerize N molecules is simply $N - 1 \approx N$ (for large N), the predicted areal density of C that is in the form of polymerized material is then given by $N_C = H_{C-C}n_C$, where again n_C is the number of C atoms per molecule. Assuming $n_C = 24$ for dioctyl phthalate, $N_C = 8.11 \times 10^{16}$ cm^{-2}, which is ∼1% of the areal density of the contaminant present at the center of OBFs (Figure 1).

3.3 UV Fluence from Stars

The next source of UV fluence we will consider is that from bright stars. We first examined O stars which have tabulated fluxes in the International Ultraviolet Explorer (IUE) data archive[2] with apparent magnitudes of 6 or less which have also been observed by *Chandra*. We also chose to examine the UV flux from other stars which were observed by *Chandra* by filtering on the "Stars and WD" Science Category of the *Chandra* Data Archive, and which also have tabulated spectra in the IUE archive. In both cases, we only examined sources which fell witin 1' of the aimpoint for that observation, and were not observed with the HETG in, because the transmissivity of the HETG to UV photons is very low. The transmissivity of the LETG to UV photons is ∼50%, so observations with the LETG in were weighted accordingly. The list of stars that were examined, their UV fluxes, and the *Chandra* exposure times are given in Table 1. The most significant UV fluences in this sample are from the stars of the Trapezium Cluster, which has been observed by *Chandra* for ∼1 Ms.

In keeping with our "worst case" approach, we assume that each source is observed at the aimpoint and that the UV fluence is spread out over an area on the OBFs corresponding to the outline of the standard *Chandra* dither pattern of 32×32 pixels, or ∼248 square arcseconds. For each source, we integrate over the UV flux shortward of 3445 Å (the energy required to break C-C bonds), down to ∼1150 Å, the lower-wavelength limit of IUE.

Summing the contributions from all of our sources together, and using Equation 3 we find a total fluence of $H = 1.09 \times 10^{16}$ photons cm^{-2}. As for the previous calcuation, we can determine the predicted areal density of polymerized contaminant, assuming 100% efficiency. Using the same formalism as above, we find $N_C = 2.61 \times 10^{17}$ cm^{-2}, ∼4% of the areal density of the contaminant present at the center of the OBFs, which is slightly higher than the predicted amount resulting from the bright Earth.

---

[2]https://archive.stsci.edu/iue/

Table 1: UV Fluxes and Exposure Times for Bright UV Stars

Star	Flux (1150-3445 Å, photons s^{-1} cm^{-2})	Exposure Time (ks)
HD172167*	9.62×10^5	38.00
HD37468	3.94×10^5	12.96
HD36861	3.92×10^5	9.46
HD57061	1.56×10^5	97.88
HD38666	1.47×10^5	115.81
HD37022†	1.02×10^5	1040.00
HD37020†	1.94×10^4	1040.00
HD37023†	1.76×10^4	1040.00
HD135379	1.42×10^4	19.05
HD152248	1.07×10^4	120.57
HD91969	1.06×10^4	70.87
HD37021†	5.37×10^3	1040.00
HD24534	5.23×10^3	111.09
HD46150	5.01×10^3	75.00
HD124314	4.58×10^3	27.90
HD193793	9.06×10^2	79.60

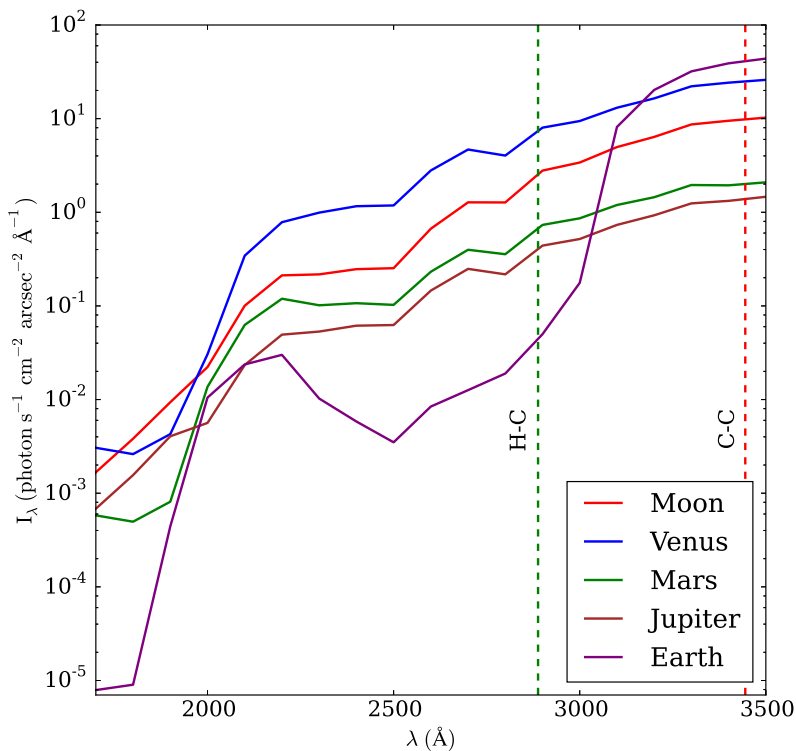* Vega
† Trapezium star cluster

Figure 4: Specific intensity of solar UV photons backscattered from solar system objects which have been observed by *Chandra*, along with the Earth. Dashed vertical lines show the wavelengths of photon energies that can break H-C and C-C bonds.

3.4 UV Fluence from Solar System Objects

The last source of UV fluence we will consider is that from solar system objects. *Chandra* has observed the Moon, Venus, Mars, and Jupiter, all of which are at least potentially bright in the UV. Figure 4 shows the intensity of solar UV photons reflected from the Sun for these objects, with that from the Earth plotted for comparison (provided by Randy Gladstone of SwRI via Peter Ford of MIT).

For this calculation, we assume that each solar system object was observed at the same aimpoint and that the object did not move in the field of view, again consistent with our "worst-case" approach. We further assume that each object was always observed at full phase, relevant for Venus and the Moon. The total exposure of these different solar system objects by *Chandra* and their UV intensities are tabulated in Table 2.

Using the same procedure as Sections 3.2 and 3.3, we find the total predicted areal density the form of polymerized contaminant resulting from the UV fluence from all solar

Table 2: UV Intensities and Exposure Times for Solar System Objects

Object	Intensity (1000-3500 Å, photons s^{-1} cm^{-2} arcsec^{-2})	Exposure Time (ks)
Moon	1.70×10^{11}	33.00
Venus	4.69×10^{11}	251.42
Mars	4.19×10^{10}	65.03
Jupiter	2.61×10^{10}	350.98

system objects is $N_\mathrm{C} = 3.25 \times 10^{18}$ cm^{-2}, $\sim$44% of the areal density of the contaminant present at the center of OBFs. We find that $\sim$87% of this estimate is from the $\sim$250 ks of Venus observations, which is expected given the relative brightness of Venus in the UV shown in Figure 4 and the amount of time that it has been observed.

This predicted areal density of polymerized contaminant is a significant fraction of the measured areal density, which implies that it should be investigated further. To obtain a more accurate estimate of the UV fluence, it will be necessary to relax one or more of our assumptions. The easiest and most relevant assumptions to relax are that Venus was observed at the same aimpoint for every observation and that it did not move in the field of view. Therefore, we will need to calculate the fluence of UV photons from Venus as a function of position on the ACIS OBFs, which we detail in the next section.

3.4.1 Detailed Calculation of the UV Fluence from Venus

We first identify all of the observations of Venus by ACIS in the Obscat, which are shown in Table 3. In our calculations, we will include the contribution to the UV fluence from all of these observations, excepting the two short ACIS-S observations with LETG (OBSIDs 2411 and 2414), which reduces the UV transmission by $\sim$50%. The remaining observations are all with ACIS-I and no gratings, and are roughly 250 ks of exposure in total.

We use the aspect solution from each observation to obtain a set of time intervals over which to compute the fluence. These time intervals are fed into AstroPy's `get_body`[3] function which obtains the ephemeris for Venus at these times, including the right ascension, declination, and Earth-Venus distance. We use these celestial coordinates as input to the CIAO tool `dmcoords`[4], together with the aspect solution, to compute the `CHIPX`, `CHIPY`, and `CHIP_ID` for each time interval to determine the position of the center of Venus on the ACIS I-array as a function of time. The angular size of Venus on the I-array as a function of time is determined via the Earth-Venus distance and the radius of Venus. Figure 5 shows an example track of the Venus position and size across the I-array for OBSID 9753.

---

[3]`http://docs.astropy.org/en/stable/api/astropy.coordinates.get_body.html`
[4]`http://cxc.harvard.edu/ciao/ahelp/dmcoords.html`

Table 3: ACIS Venus Obsservations

| OBSID	Instrument	Grating	Exposure Time (ks)	Start Date/Time
583	ACIS-I	NONE	11.71	2001-01-13 12:22:12
2411	ACIS-S	LETG	5.86	2001-01-10 19:13:49
2414	ACIS-S	LETG	5.68	2001-01-10 21:13:08
6395	ACIS-I	NONE	6.20	2006-03-27 04:09:42
7306	ACIS-I	NONE	6.25	2006-03-27 06:12:11
7307	ACIS-I	NONE	6.25	2006-03-27 08:04:01
7308	ACIS-I	NONE	6.24	2006-03-27 09:55:51
7309	ACIS-I	NONE	6.25	2006-03-27 11:47:41
7310	ACIS-I	NONE	6.25	2006-03-27 13:39:31
7311	ACIS-I	NONE	6.25	2006-03-27 15:31:21
7312	ACIS-I	NONE	6.25	2006-03-27 17:23:12
7313	ACIS-I	NONE	6.25	2006-03-27 19:15:01
7314	ACIS-I	NONE	6.25	2006-03-27 21:06:51
7315	ACIS-I	NONE	6.25	2006-03-27 22:58:41
7316	ACIS-I	NONE	6.25	2006-03-28 00:50:31
7406	ACIS-I	NONE	6.58	2007-10-29 21:34:27
9741	ACIS-I	NONE	6.64	2007-10-29 23:47:48
9742	ACIS-I	NONE	6.63	2007-10-30 01:46:17
9743	ACIS-I	NONE	6.63	2007-10-30 03:44:48
9744	ACIS-I	NONE	6.73	2007-10-30 05:43:18
9745	ACIS-I	NONE	6.74	2007-10-30 07:43:28
9746	ACIS-I	NONE	6.73	2007-10-30 09:43:38
9747	ACIS-I	NONE	6.74	2007-10-30 11:43:48
9748	ACIS-I	NONE	6.72	2007-10-30 13:43:58
9749	ACIS-I	NONE	6.74	2007-10-30 15:44:07
9752	ACIS-I	NONE	6.73	2007-10-30 17:44:18
9753	ACIS-I	NONE	6.73	2007-10-30 19:44:28
15292	ACIS-I	NONE	8.76	2013-11-08 03:29:57
16499	ACIS-I	NONE	8.86	2013-11-08 06:23:23
16500	ACIS-I	NONE	8.85	2013-11-08 09:00:13
16501	ACIS-I	NONE	7.96	2013-11-08 11:37:03
16502	ACIS-I	NONE	8.81	2013-11-08 14:13:53
16503	ACIS-I	NONE	8.86	2013-11-08 16:50:43
16504	ACIS-I	NONE	8.86	2013-11-08 19:27:33
16505	ACIS-I	NONE	8.85	2013-11-08 22:04:23
16506	ACIS-I	NONE	8.76	2013-11-09 00:41:13
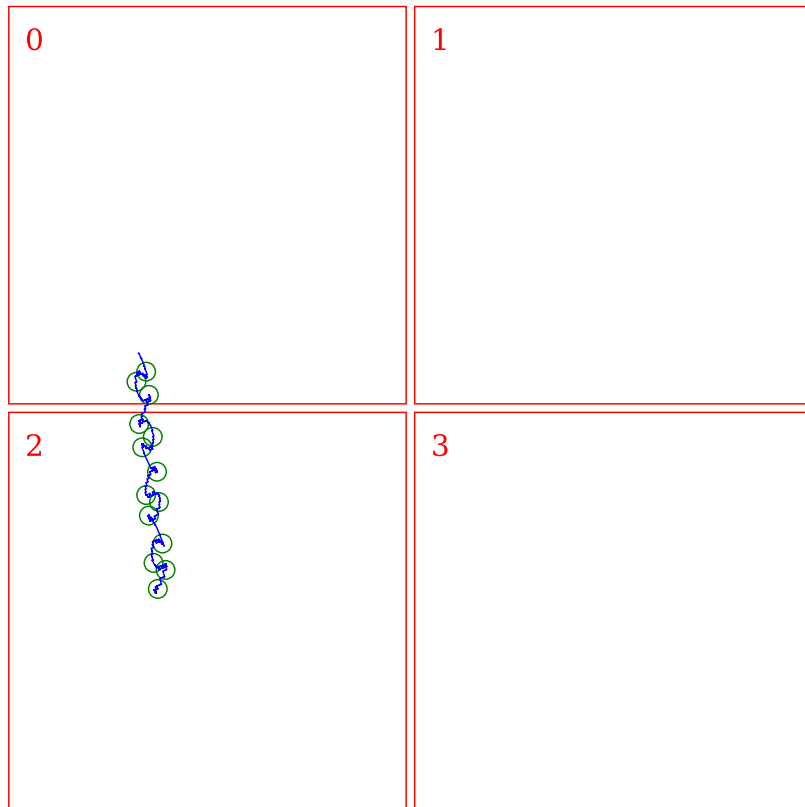
Figure 5: Example track of Venus across the I-array for OBSID 9753, clearly showing the dithering pattern superimposed on its proper motion across the sky. Green circles represent the angular size of Venus.
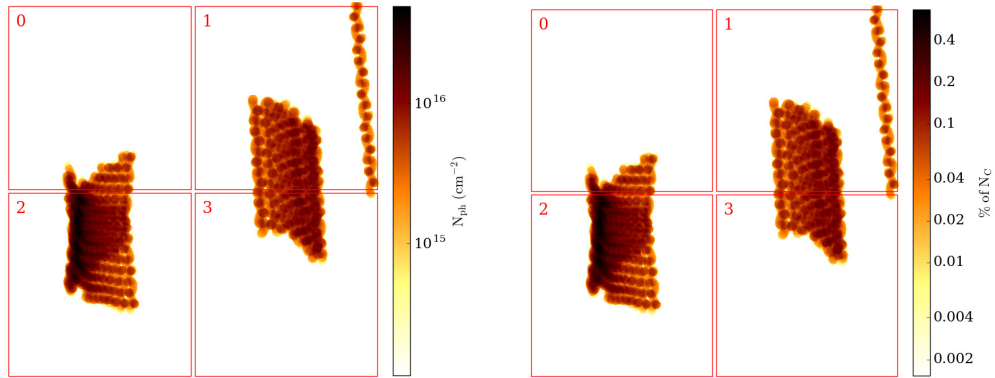
Figure 6: Predicted amounts of polymerized contaminant from all ACIS-I observations of Venus in Table 3. Left: Predicted areal density of polymerized contaminant. Right: The predicted percentage of the contaminant that is polymerized.

We use the same measure of the UV intensity from Venus from Section 3.4 to compute the fluence on the OBFs for each observation, which are added in total to provide a total predicted areal density of polymerized contaminant, shown in Figure 6. We see that the UV fluence from Venus is concentrated mostly on I2 and I1, with smaller amounts on I0 and I3. The predicted areal density of polymerized contaminant from these observations is small everywhere, reaching only up to ∼0.5% of the measured areal density of the contaminant at its highest level.

3.4.2   UV Fluence from the Io Plasma Torus

We also briefly considered the fluence in the EUV band from the plasma torus surrounding Jupiter at the orbit of its moon Io. The Cassini spacecraft measured the EUV spectrum of the Io plasma torus in the year 2000. The EUV spectrum of the Io plasma torus in the wavelength range of 561-1181 Å is shown in Figure 5 of Steffl et al. 2004.

We can use this EUV spectrum to compute the UV fluence received from the Io plasma torus during the ∼350 ks that *Chandra* observed Jupiter. All of the photons in the observed wavelength range are capable of polymerizing C-C and H-C bonds. Carrying out the same calculations as in the previous sections, we find that the predicted areal density of polymerized contaminant from observing the Io plasma torus is $N_C = 3.67 \times 10^{12}$ cm^{-2}, many orders of magnitude smaller than the contributions from the other sources, so it can be safely ignored.

3.5 Fluence from the Local UV Background

Finally, we consider the fluence accumulated over the lifetime of the mission from the local UV background.

4 Summary

We have presented a series of calculations of the estimated UV fluence which has impinged on the ACIS OBFs over the lifetime of the mission from various sources, and the predicted areal density of polymerized contaminant that results. The following limitations of our study must be kept in mind:

- Throughout this memo, we assumed that sufficiently energetic UV photons polymerize contaminant with 100% efficiency, which is not likely to be the case.

- We have not considered other sources of UV fluence, such as diffuse sources which have been observed by *Chandra*. Based on preliminary calculations, we do not believe these to be significant sources of UV fluence.

- We have assumed that the HRMA is 100% reflective to UV photons.

- We have assumed (with the exception of the Venus observations) that all of the UV fluence is observed at the same aimpoint. In reality, most of the observations have been taken with the aimpoint near the center of the I-array and on the S3 chips. There should be even less UV fluence on other areas of ACIS.

We are confident that relaxing some of these assumptions and adopting more detailed calculations will not change our conclusions, since most of these assumptions result in an *overestimate* of the polymerization of the contaminant. Though it is inevitable that some of the contaminant on the ACIS OBFs must be in polymerized form, we conclude from the calculations presented in this memo that the amount of contaminant that is polymerized is at most on the few percent level.

5 References

Feinberg, L., Chivatero, C., Colony, J., et al. 1995, "Wide Field/Planetary Camera-I Pick-off Mirror Contamination Failure Review Board Report."

Marshall, H. L., Tennant, A., Grant, C. E., et al. 2004, Proceedings SPIE, 5165, 497

O'Dell, S. L., Swartz, D. A., Tice, N. W., et al. 2015, Proceedings SPIE, 9601, 960107

Plucinsky, P. P., Bogdan, A., Germain, G., & Marshall, H. L., Proceedings SPIE, 9905, 990544

Steffl, A. J., Stewart, A. I. F., & Bagenal, F. 2004, Icarus, 172, 78